FULL PAPER

Layer-Controlled and Wafer-Scale Synthesis of Uniform and High-Quality Graphene Films on a Polycrystalline Nickel Catalyst

*Youpin Gong, Xuemin Zhang, Guangtong Liu, Liqiong Wu, Xiumei Geng, Mingsheng Long, Xiaohui Cao, Yufen Guo, Weiwei Li, Jianbao Xu, Mengtao Sun, Li Lu, and Liwei Liu**

Chemical vapor deposition (CVD) provides a synthesis route for large-area and high-quality graphene films. However, layer-controlled synthesis remains a great challenge on polycrystalline metallic films. Here, a facile and viable synthesis of layer-controlled and high-quality graphene films on wafer-scale Ni surface by the sequentially separated steps of gas carburization, hydrogen exposure, and segregation is developed. The layer numbers of graphene films with large domain sizes are controlled precisely at ambient pressure by modulating the simplified CVD process conditions and hydrogen exposure. The hydrogen exposure assisted with a Ni catalyst plays a critical role in promoting the preferential segregation through removing the carbon layers on the Ni surface and reducing carbon content in the Ni. Excellent electrical and transparent conductive performance, with a room-temperature mobility of ≈3000 cm^2 V^{-1} s^{-1} and a sheet resistance as low as ≈100 Ω per square at ≈90% transmittance, of the twisted few-layer grapheme films grown on the Ni catalyst is demonstrated.

1. Introduction

Graphene, a two-dimensional monolayer consists of a hexagonal crystal structure of sp^2-bonded carbon atoms, has been attracting intense interests due to its unique structure and exceptional physical properties.[1–4] Recently emerging chemical vapor deposition (CVD) technique using Cu or Ni as catalysts exhibits great advantages in large-area synthesis of near-perfect graphene.[5–9] The layer-controlled surface growth of large-area graphene films has been actively pursued for their distinct properties and diverse applications, as well as compatibility with manufacture technologies.[10–12] The large-area film,[5] the excellent transparent conductor[6] and the large domain sizes[13,14] of uniform graphene have been demonstrated on Cu foil at low pressure. However, layer-controlled graphene films with high uniformity are to be further investigated owing to its surface self-limited nature on Cu foils in the growth process,[15,16] although the self-limited growth has been broken by using liquid carbon precursor.[17,18] Compared with Cu, despite thin Ni film used, the produced graphene films are random distribution with the non-uniform thickness from one to a few tens of layers due to the larger carbon solubility in Ni.[15,19]

For conventional CVD graphene films (CVDG) on Ni surface, the process generally involves the dissociation of the hydrocarbon, the dissolution and diffusion of carbon in Ni and the formation of graphene. The formation of graphene films probably contains the several dynamic processes: metal-induced crystallization at high temperature,[20,21] segregation at the interface and precipitation at grain boundaries during cooling.[15] Intertwinement of these complicated processes, especially the precipitation at grain boundaries, will result in the non-uniformity and the uncontrollable layers of graphene films. Aiming at these problems, the pioneer segregation growth of graphene has been employed on Ni foils.[22] Additionally, the uniformity and quality of graphene has subsequently been improved by a sole segregation under vacuum annealing using the carbon-containing metal catalyst films.[23] However, the layer-controlled synthesis of large-area and high-quality graphene films on polycrystalline Ni catalyst has not been solved by previously reported segregation methods.

Here, we develop a remarkable synthesis technique to achieve layer-controlled and high-quality graphene films on wafer-scale Ni films at ambient pressure by creating a hydrogen (H$_2$) exposure process. The schematic diagrams illustrate the synthesis processes of the segregated graphene films involving gas carburization, H$_2$ exposure and segregation (CVDSG) (**Figure 1**; also see Figure S1, Table S1, and the details in Supporting Information). H$_2$ exposure assisted by Ni film at high temperature plays critical roles not only in the removal of the

Dr. Y. P. Gong, X. M. Zhang, Dr. L. Q. Wu,
Dr. X. M. Geng, M. S. Long, X. H. Cao, Y. F. Guo,
W. W. Li, J. B. Xu, Prof. L. W. Liu
Key Laboratory of Nanodevices and Applications
Suzhou Institute of Nano-tech and Nano-bionics
Chinese Academy of Sciences
398 Ruoshui Road, Suzhou, Jiangsu 215123, P. R. China
E-mail: lwliu2007@sinano.ac.cn
Prof. G. T. Liu, Prof. M. T. Sun, Prof. L. Lu
Institute of Physics
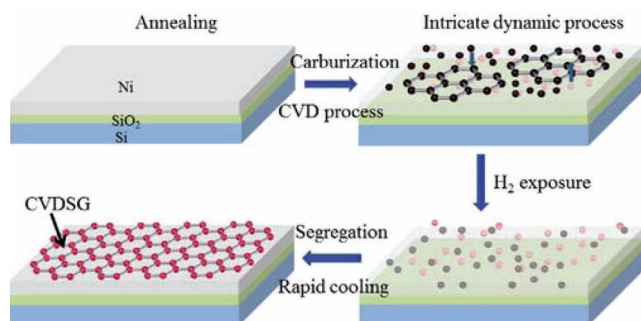Chinese Academy of Sciences
Beijing 100190, P. R. China

Figure 1. Schematic diagrams of synthesis processes of CVDSG films. First, the Ni/SiO$_2$/Si substrates are annealed in the tube furnace under ambient pressure by flowing H$_2$ and Ar. Then, the gas carburization is performed by CVD using CH$_4$ as carbon source. Subsequently, the sole H$_2$ exposure is applied after stopping carbon supply. Finally, the isolated segregation produces highly uniform graphene films on Ni surface by rapid air cooling.

carbon layers formed in the initial CVD carburization process but also in the effective reduction of the carbon mount in Ni for promoting the sequential segregation process. The number of layers is precisely controlled by changing Ni film thickness, gas carburization amount and H$_2$ exposure dose. We demonstrate the outstanding electrical and transparent conductive performance of the few-layer graphene films.

2. Results and Discussion

The optical image comparisons indicate that the CVDSG films are considerably uniform as compared to the CVDG films (**Figure 2**a–f and Figure S2, Supporting Information). For CVDG on Ni films (Figure 2a–c and Figure S2a–c, Supporting Information), the obvious non-uniformity of the CVDG films with random thicker graphene multilayers (dark regions) are
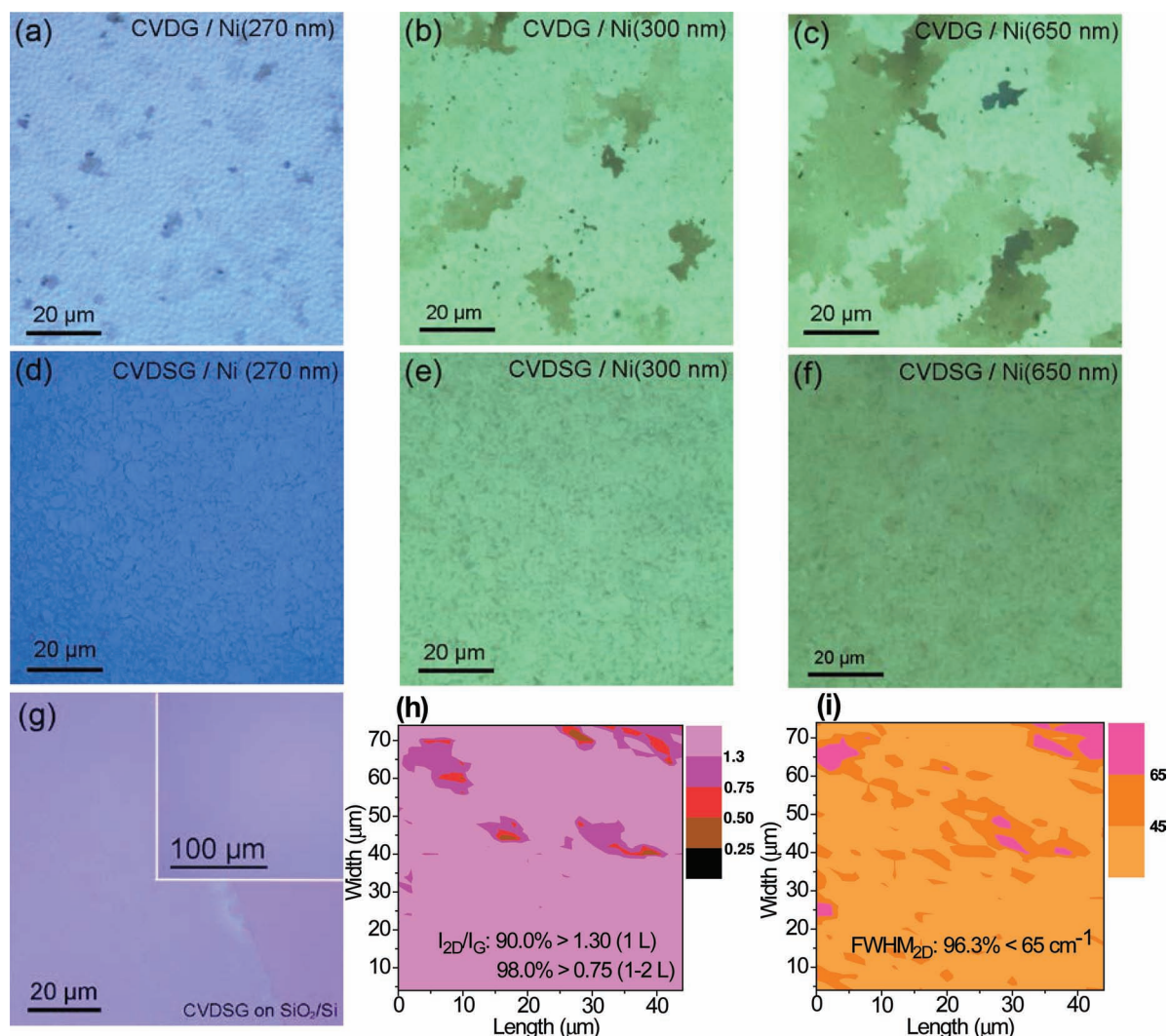

Figure 2. Comparison of uniformity between conventional CVD-graphene (CVDG) and segregated-graphene (CVDSG). a–f) Optical images of CVDG (a–c) and CVDSG (d–f) on Ni film substrates with different thicknesses. The apparent non-uniformity of the CVDG films and the random distribution of thick graphene multilayers are observed by the changes of color contrast (a–c). In contrast, the optical contrast variations of the CVDSG samples are negligible, which indicates that the CVDSG films are relatively uniform (d–f). g) Optical images of the same CVDSG film in (d) transferred onto SiO$_2$ (300 nm)/Si substrates. The inset in (g) shows corresponding high-magnification optical image. h,i) I_{2D}/I_G (h) and W_{2D} (i) Raman mapping of CVDSG films (1–2 layers) on an area of 44×70 μm^2.

observed according to the changes of color contrast. In contrast, the optical contrast variations of the images from the CVDSG samples (Figure 2d–f and Figure S2d–f, Supporting Information) are negligible, in addition to the grain boundaries of the Ni film over the entire surface, which indicates that the CVDSG films are of uniform thickness. The optical images of the same CVDSG film in Figure 2d transferred to SiO_2/Si substrates further confirm the uniformity. The highly uniform graphene films can be formed even on the thicker Ni films, i.e., 650-nm-thick and 1-μm-thick Ni films (Figure 2f and Figure S2e,f, Supporting Information), suggesting the suppression of the precipitation of carbon. The 2D to G peak ratio (I_{2D}/I_G) and 2D-band full-width

at half-maximum (FWHM, W_{2D}) Raman mapping of monolayer/bilayer CVDSG (44×70 μm^2) are shown in Figure 2h,i. The determination of graphene layer number is based on the I_{2D}/I_G values combining with the W_{2D} (see the details in Supporting Information). The coverage of ~90% monolayer with ~6% bilayer CVDSG is obtained in the measured regions, which is comparable to that of CVD-grown monolayer graphene on Cu foils.[5] High uniformity of the CVDSG films is further confirmed by the stochastic observations of high-resolution transmission electron microscopy (HRTEM) (Figure S3, Supporting Information). Furthermore, the wafer-scale CVDSG films are successfully synthesized and transferred (**Figure 3**a and the insets in Figure 3a).
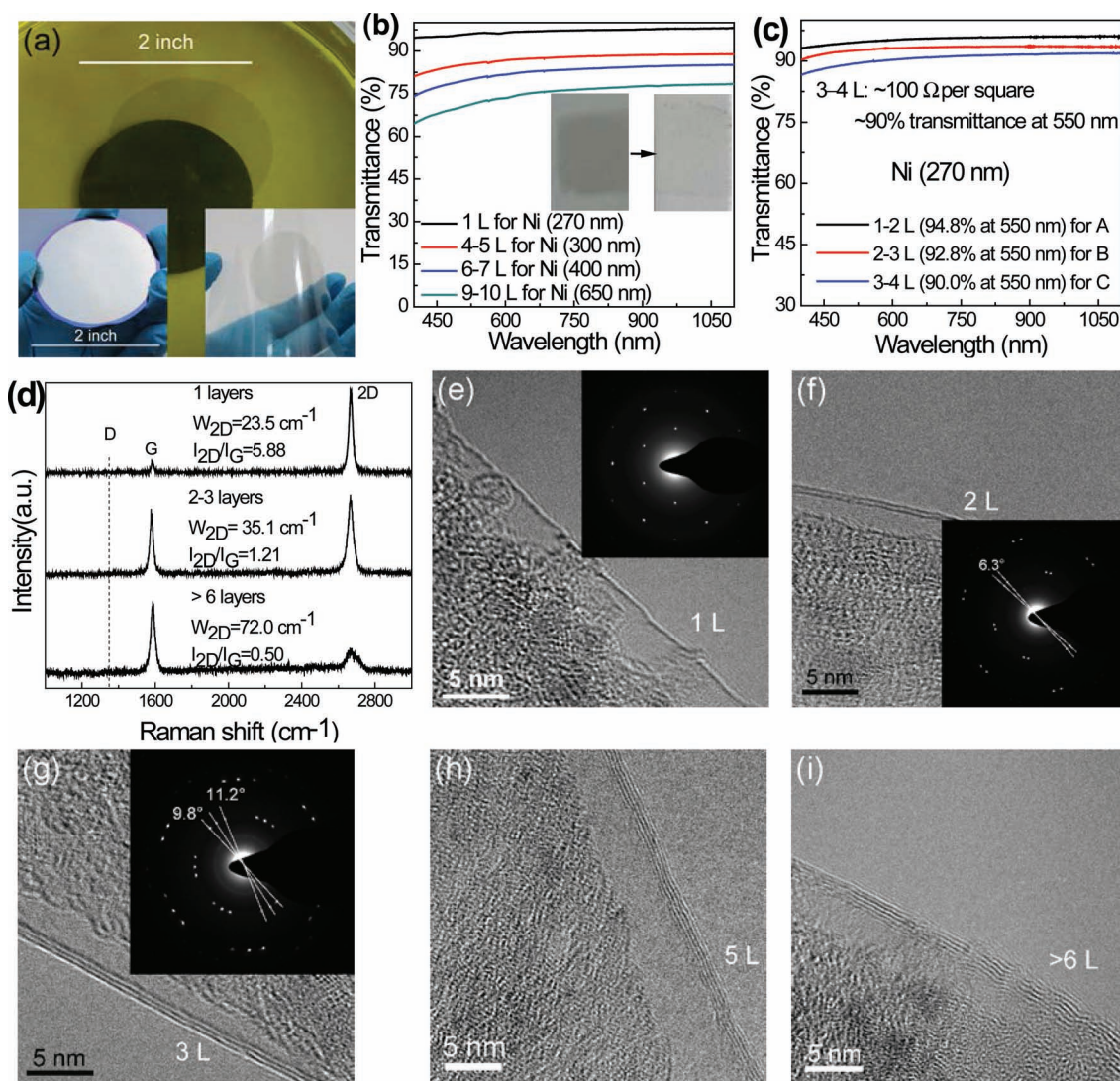

Figure 3. Various spectroscopic and HRTEM characterizations of the CVDSG. a) 2-inch graphene film (left inset) is released in the deionized water after etching the Ni film with a mild FeCl$_3$ aqueous solution (1 mol/l) and is transferred onto the PET flexible substrates (right inset). b) Optical transmittance of CVDSG films obtained from Ni films with various thicknesses. The inset shows the photographs of CVDSG films on glass slide with ~90.0% up to ~96.4% transmittance at 550 nm. c) Optical transmittance of CVDSG films derived from 270-nm-thick Ni film. See Experimental Section for the recipes for samples A, B, and C. d) Raman spectra of CVDSG films. For the sample with ~96.4% transmittance, its symmetric 2D-band peak shows a single Lorentzian feature with a small W$_{2D}$ of ~23.5 cm^{-1} and a high I$_{2D}$/I$_G$ ratio (5.88), which is consistent with hallmarks of a single-layer graphene. e–i) HRTEM images of CVDSG and their corresponding SAED (insets in (e–g)). In real space, the twist angle α can be calculated by $\alpha = 60° - 2\theta$, where θ is rotation angles in k-space. If $\alpha > 30°$, the twist angle in real space should be $60° - \alpha$.

ADVANCED
FUNCTIONAL
MATERIALS
www.afm-journal.de

Materials
Views
www.MaterialsViews.com

The precise control over the number has been achieved by modulating the Ni film thickness, CVD carburization parameters (temperature, gases flow, and time), and the H_2 exposure dose. The thickness control of the uniform CVDSG films is determined by HRTEM and ultraviolet-visible (UV-Vis) spectrum according to the absorbance of ~2.3% each layer.[24] We found that the Ni film thickness is a major factor for large-range control over the layer number of CVDSG films ranging from 1 to 10 layers (L) (Figure 3b). We also fabricate the CVDSG films with different layer numbers on 270-nm-thick Ni films by changing growth recipe such as carburization time, H_2 exposure time and flow rate (sample A–C in Figure 3c). Moreover, we can obtain a single-layer CVDSG by employing the 270-nm-thick Ni combining with the tune of the synthesis recipe (see Figure 3b,c and Table S1, Supporting Information). Obviously, when the Ni thickness is less than ~300 nm, the segregation growth parameters can effectively tune the CVDSG layer number ranging from 1 to 4 L (Figure 3c). The HRTEM images of the fabricated CVDSG show single-layer, few-layer and multi-layer graphene, respectively (Figure 3e–i), which are consistent with that calculated from their optical transmittance. The 3–4 L CVDSG films without multiple transfers show the high performance of the transparent conductor, the sheet resistance of as low as ~100 Ω per square measured by a four point method at ~90% transmittance at 550 nm (Figure 3c), which is comparable to commercial indium tin oxides transparent electrodes.

Micro-Raman spectra are employed to characterize the layer numbers, the quality and the stacking arrangements of CVDSG films (Figure 3d and Figure S4, Supporting Information). The D peaks at ~1350 cm^{-1} are small or negligible even for our

thicker CVDSG films, suggesting the sparsity of disorders such as defects and grain boundaries.[25,26] Both single and few-layer graphene (2–3 L) show single Lorentzian lineshapes of 2D-band with the low W_{2D} value, indicating that 2–3 L graphene exhibits a disordered AB stacking between layers without electronic coupling.[27] The twisted layers in our 2–3 L CVDSG film are also verified by selected area electron diffraction pattern (SAED) (see the insets in Figure 3f,g). Two kinds of twist angle of 19.6° and 22.4° in real space have been found in a 3 L CVDSG film. The results imply that our 2–3 L CVDSG exist the electronic properties similar to monolayer graphene due to the decoupling of layers with the large twist angle.[28]

In order to elucidate the roles of in situ H_2 exposure in synthesis process, we carried out experiments of gradually extending the H_2 exposure time before the segregation stage. The thickness of the prepared CVDSG films is reduced and eventually the graphene films disappear on the surface (**Figure 4**a–c), as determined by the Raman spectra (Figure 4d). The etching role of H_2 with the assistant of Ni catalytic film at high temperature has been further approved by ex situ H_2 exposure on as-grown CVDG films (Figure S5, Supporting Information). For further understanding H_2 etching and CVDSG growth process, we overly increase the amount of carburizing and purposely reduce the dose of H_2 exposure, and the thicker and uneven carbon layers can survive in partial region (Figure 4e,f). The large fluctuation of layer number ranging from 2 to more than ten layers appears in the thicker layer region (Figure 4g), while relatively uniform and 2–3 L graphene layers (Figure 4h) occur in the other region similar to CVDSG. The observation suggests the synergistic etching
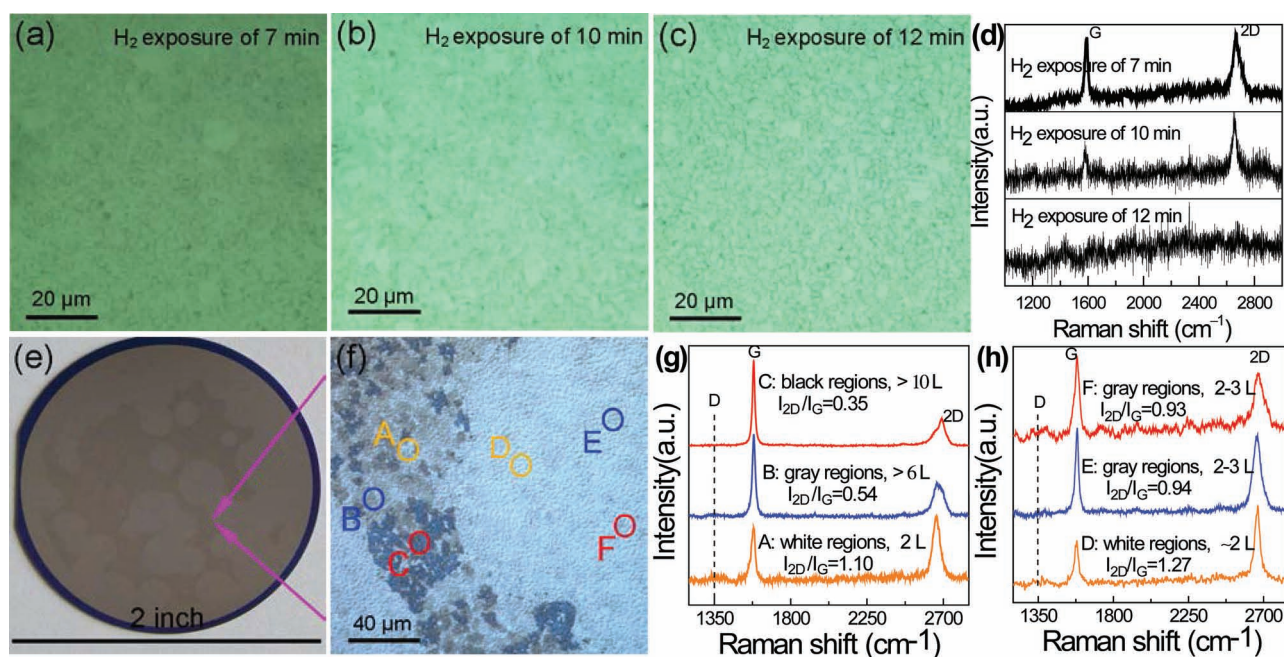

Figure 4. H_2 etching effect and CVDSG growth mechanism. a–c) Optical images of graphene on Ni films with in situ H_2 exposure (before segregation stage) of 7, 10, and 12 min, respectively. d) Raman spectra obtained from CVDSG with various H_2 exposure time. e) The thicker and uneven carbon layers can survive in partial region (dark region) on the 2-inch Ni surface. f) A magnified optical image of the location identified by the arrow in (e). The dark region shows a typical optical morphology with non-uniformity. g,h) Raman spectra from the thicker layer region (indicated spots: A-orange, B-blue and C-red) and the other region similar to CVDSG (marked locations: D-orange, E-blue and F-red) shown in (f), respectively.

www.MaterialsViews.com

ADVANCED
FUNCTIONAL
MATERIALS
www.afm-journal.de

FULL PAPER

effect of H_2 and Ni film may start from the regions with the thinner carbon layers or some defects in the grain boundaries (also see the details of Figure S5, Supporting Information). The CVDG-like thick carbon layers are remained due to the incomplete etching, indicating that the original carbon layers can be formed during the CVD carburization process. The thicker and non-uniform carbon layers are a combination of the original carbon layers interacting with subsequent segregation or precipitation. Therefore, it is concluded that the original crystalline graphene films on the Ni surface grown by the carburization process can be dissolved and removed by the synergistic effect of H_2 and Ni film. Moreover, in the dynamic diffusion process, the amount of carbon in the bulk Ni film also can be reduced by the H_2 etching of carbon atoms diffusing outward the Ni surface from the bulk Ni. This leads to the layer controls or the absence of the CVDSG films in our experiments. According to the temperature-solubility kinetic process, the segregation is more apt to take place with a lower carbon amount and at a higher temperature than is the precipitation.[29,30] The reduced amount of carbon along with high temperature strongly suppresses the precipitation of carbon at grain boundaries.

We also investigate the effect of ex situ H_2 exposure on as-grown CVDSG films (**Figure 5**) and segregation temperatures in growth process (Figure S6, Supporting Information). Firstly, the uniform few-layer CVDSG film is fabricated on Ni (300 nm) surface by our segregation process (see Figure 5a). Subsequently, the sample is inserted again to the furnace and exposed to H_2 (400 sccm) for 5 s at 900 °C (Figure 5b,c). The narrow dark regions (see Figure 5b,c) represent the bare Ni substrate, indicating that the CVDSG film in these regions is etched by H_2. Interestingly, the comparison results of the ex situ H_2 etching are remarkably different between CVDSG film and CVDG film (Figure 5 and Figure S5, Supporting Information). The etching traces of CVDSG films show a number of hexagonal trenches and the domains of ~400 μm are leaved with a large portion of hexagonal edges. The crystallographic orientation-dependent etching effect of hydrogen has been recently shown in graphene films.[31,32] The coincidence of the topological shapes and domain sizes in the control experiments of the segregation temperature (see Figure S6, Supporting Information) and the

ex situ H_2 etching suggests that the CVDSG films are made of random domains with the size of ~400 μm. The relative regular hexagonal grain and the large grain size are comparable to that of graphene on Cu foils,[14] which have not yet been observed in previous CVD graphene grown on Ni film.

According to our performed etching experiments of CVDG and CVDSG, we assume the reasonable explanation is that etching process starts readily from the graphene layer directly contacted to Ni film, especial positions at the vulnerable grain boundaries and defects. Additionally, the etching can proceed from both bottom contact and lateral orientation. Anisotropic etching picture is understood that the vulnerable part of the bottom contact is dissolved firstly, and then the second layer collapses on the Ni. Therefore, under the synergistic role of H_2 and Ni film, we can see that the etched trenches in CVDSG are formed and widened gradually (Figure 5). For non-uniform CVDG film, it has more concentration of the grain boundaries, and the etching forms some circular holes for the vulnerable positions are firstly etched out. The density and area of the holes increase with etching time due to above-mentioned dual etching roles (Figure S5, Supporting Information).

To evaluate the electrical properties of our segregated few-layer graphene, the 3–4 L CVDSG films are patterned into Hall bar devices by standard photolithography, and the electronic transport measurements are carried out (**Figure 6**, Figure S7, Supporting Information). All samples show high level of hole-doping in the order of 10^{13} cm^{-2}, and the Dirac point is not observed even at gate voltages of up to 70 V. The high doping level and the screening of the few-layer graphene are responsible for the unavailability of Dirac point by gating. Owing to high carrier concentration, the Landau level index near Fermi level is large, hence, it is hard to observe the quantum Hall effect (QHE) feature except the weak Shubnikov-de Has oscillations (SdHOs) in longitudinal resistance (Figure 6b). The carrier concentration derives from the low-field linear slope of Hall resistance R_{xy} against magnetic field, $n_p = 1/e \left(d R_{xy} / d B \right)$, and the mobility is obtained by $\mu = (L/W)(e n_p R_{xx})^{-1}$. The concentration of our CVDSG sample is estimated to be 1.4×10^{13} cm^{-2} at zero gate voltage, and the mobility is ~5400 and ~2900 cm^2 V^{-1}s^{-1} at 0.36 and 300 K, respectively. The p-type doping is
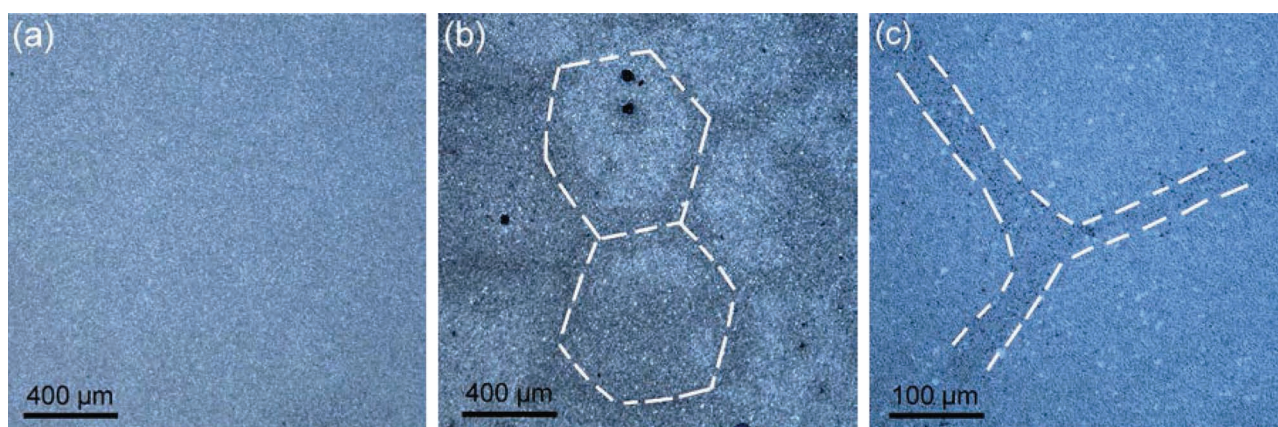

Figure 5. The effect of H_2 etching on CVDSG films by ex situ H_2 exposure (400 sccm) at 900 °C. a) Optical images of as-grown CVDSG films on Ni films. b,c) Optical images of ex situ H_2 exposure for CVDSG films (the sample in (a)) on Ni films (dashed lines mark the etching traces). The narrow dark regions (b,c) represent the bare Ni substrate.
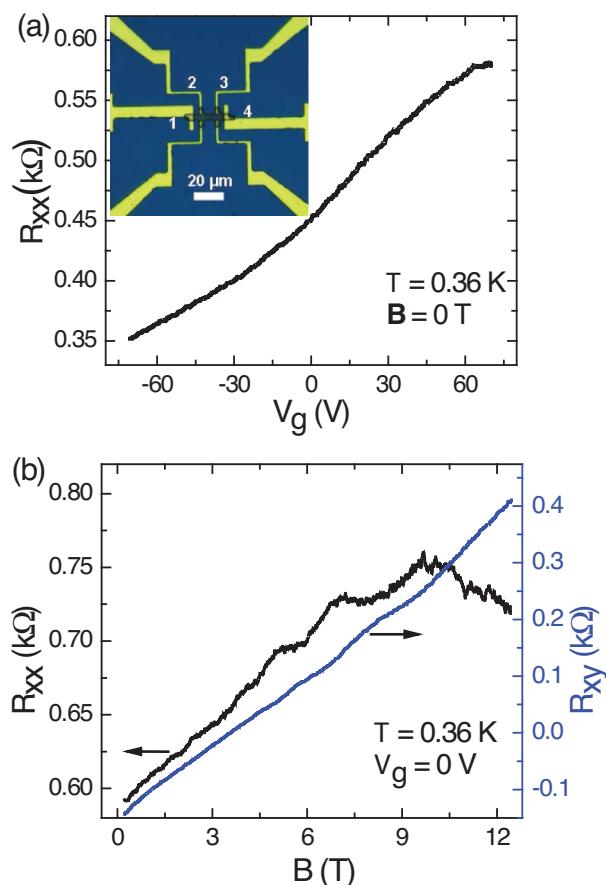
Figure 6. Electrical properties of CVDSG. a) Four-probe electrical longitudinal resistance (R_{xx}) versus gate voltage (V_g) measured in a graphene Hall bar device (inset) at the temperature (T) of 0.36 K. b) R_{xx} and R_{xy} (transverse magnetoresistances) as functions of magnetic field (B) measured at $T = 0.36$ K and $V_g = 0$ V. The device demonstrates the weak Shubnikov-de Has oscillations (SdHOs) in longitudinal resistance ($L = 12$ μm, $W = 3$ μm).

likely caused from the residue of Ni etchant for the p-type remains avoiding photoresist and lithography process. The mobilities for our CVDSG are comparable to previous reports on CVD-grown monolayer graphene films, and are higher than that of non-twisted bilayer and trilayer graphene films on SiO_2 substrates made by mechanical cleavage and CVD growth.[5–9] Our electrical measurement confirms that the electrical quality of twisted few-layer CVDSG films approaches monolayer graphene, in agreement with the recent conclusion of scanning tunneling spectroscopy (STS) experiments.[28]

3. Conclusions

In conclusion, we have developed a novel growth technique to readily synthesize wafer-scale, layer-controlled and highly uniform graphene films by creating a H_2 exposure process. The layer number of CVDSG films can be precisely controlled by changing the Ni film thickness, carburization parameters and the H_2 exposure dose. H_2 exposure assisted

by nickel film at high temperature plays a critical role on the layer control and uniformity of our CVDSG films. The excellent electrical and transparent conductive performance of CVDSG has been achieved. Our findings open a feasible route towards control over the layer number of wafer-scale graphene, new understanding of the graphene formation on Ni catalyst, and eventual diverse applications of graphene-based devices.

4. Experimental Section

CVDSG Films Synthesis and Transfer: Large-area and layer-controlled graphene were synthesized on Ni films (270, 300, 400, 650 and 1000 nm) at ambient pressure by our novel technique according to a detailed description in Supporting Information (Figure S1 and Table S1). Briefly, the whole growth process consists of four stages: 1) heating and annealing; 2) carburizing; 3) H_2 exposure; and 4) purging and cooling. In addition, CVDG films on Ni film were also prepared as control samples using conventional CVD process. Samples were transferred by the wet-etching of the underlying Ni film. Firstly, the CVDSG films were protected by spin-coating poly (methyl methacrylate) (PMMA) on to the surface of graphene. Subsequently, the sample coated PMMA was released in a Ni etchant ($FeCl_3$ with 1 mol/l). The released PMMA/graphene can be easily transferred to the desired target substrates. Finally, the PMMA was dissolved and removed by acetone with 70 °C. Evaporation is observed and will be an important limitation for using thin films especially below 200 nm at such high temperature due to lower melting points of thinner Ni films. Thus, we select an optimized thickness of Ni film more than 270 nm and control the time of our CVDSG synthesis within 30 min in order to avoid the damage of the Ni film.

The CVDSG films with different layer numbers (1–4 L) on 270-nm-thick Ni films were also fabricated by changing synthesis recipe (in Figure 3c). Sample A: CVD carburization of 1.5 min by flowing CH_4 (20 sccm): H_2 (60 sccm):Ar (50 sccm), and in situ H_2 exposure of 5 min by flowing H_2 (500 sccm). Sample B: growth condition is identical to that of sample A, except higher precursor flow rate during CVD carburization (CH_4:H_2:Ar at 20:50:50 sccm) and lower H_2 exposure dose (480 sccm). Sample C: growth condition is identical to that of sample B, except longer carburization time (2 min).

Structures and Layer Number Characterization: The samples were characterized by optical microscopy, Raman spectroscopy (LabRam HR800-UV-NIR with a laser wavelength of 632.8 nm) and HRTEM (Tecnai G2 F20 S-Twin). Raman mapping were obtained from the CVDSG samples as follows: ~828 spectra collected on an area of 44 × 70 μm² with a step size of 2 μm). The TEM samples were prepared by directly transferring graphene floated on deionized water onto a TEM grid (C-flat on 200 mesh copper). The optical transmittance of CVDSG films with an area of 1×1 cm² on glass was measured by an UV-Vis spectrometer (Perkin Elmer Lambda 25). Combination of Raman spectroscopy, HRTEM and UV-Vis spectrometer was used to determine the layer number of our CVDSG films.

Device Fabrication and Electronic Transport Measurements: The CVDSG films were patterned into the Hall bar device by photolithographic. The samples were used to the electrical transport measurements by the four-terminal and the Hall probe configuration. The 3 to 4 L CVDSG films were transferred onto high doped silicon substrates with 300-nm-thick oxide layer, following 400 °C annealing at H_2/Ar gas for removal of residual PMMA. Two-step conventional photolithography processes were performed to deposit electrodes and pattern the graphene films using AZ5214 photoresist. Hall bar electrodes (electrodes of Ti/Au (20/100 nm) were deposited on the transferred graphene films by electron beam evaporation. After that, O_2 plasma etching was used to pattern 3 μm width and 37 μm length graphene stripes. The width (W) and length (L) of Hall bar are 3 μm and 12 μm, respectively. The electrical transport measurement was performed in a ³He cryostat combining with a standard lock-in technique.

Supporting Information

Supporting Information is available from the Wiley Online Library or from the author.

Acknowledgements

[1] K. S. Novoselov, A. K. Geim, S. V. Morozov, D. Jiang, Y. Zhang, S. V. Dubonos, I. V. Grigorieva, A. A. Firsov, *Science* **2004**, *306*, 666.

[2] Y. B. Zhang, Y. W. Tan, H. L. Stormer, P. Kim, *Nature* **2005**, *438*, 201.

[3] N. Tombros, C. Jozsa, M. Popinciuc, H. T. Jonkman, B. J. van Wees, *Nature* **2007**, *448*, 571.

[4] Y. M. Lin, C. Dimitrakopoulos, K. A. Jenkins, D. B. Farmer, H. Y. Chiu, A. Grill, P. Avouris, *Science* **2010**, *327*, 662.

[5] X. S. Li, W. W. Cai, J. An, S. Kim, J. Nah, D. Yang, R. Piner, A. Velamakanni, I. Jung, E. Tutuc, S. K. Banerjee, L. Colombo, R. S. Ruoff, *Science* **2009**, *324*, 1312.

[6] S. Bae, H. Kim, Y. Lee, X. F. Xu, J. S. Park, Y. Zheng, J. Balakrishnan, T. Lei, H. R. Kim, Y. Song, Y. J. Kim, K. S. Kim, B. Özyilmaz, J. H. Ahn, B. H. Hong, S. Iijima, *Nat. Nanotechnol.* **2010**, *5*, 574.

[7] K. S. Kim, Y. Zhao, H. Jang, S. Y. Lee, J. M. Kim, K. S. Kim, J. H. Ahn, P. Kim, J. Y. Choi, B. H. Hong, *Nature* **2009**, *457*, 706.

[8] A. Reina, X. Jia, J. Ho, D. Nezich, H. Son, V. Bulovic, M. S. Dresselhaus, J. Kong, *Nano Lett.* **2009**, *9*, 30.

[9] S. Lee, K. Lee, Z. H. Zhong, *Nano Lett.* **2010**, *10*, 4702.

[10] F. Schwierz, *Nat. Nanotechnol.* **2010**, *5*, 487.

[11] S. Ghosh, W. Bao, D. L. Nika, S. Subrina, E. P. Pokatilov, C. N. Lau, A. A. Balandin, *Nat. Mater.* **2010**, *9*, 555.

[12] F. N. Xia, T. Mueller, Y. M. Lin, A. Valdes-Garcia, P. Avouris, *Nat. Nanotechnol.* **2009**, *4*, 839.

[13] Q. K. Yu, L. A. Jauregui, W. Wu, R. Colby, J. F. Tian, Z. H. Su, H. L. Cao, Z. H. Liu, D. Pandey, D. G. Wei, T. F. Chung, P. Peng, N. P. Guisinger, E. A. Stach, J. M. Bao, S. S. Pei, Y. P. Chen, *Nat. Mater.* **2011**, *10*, 443.

[14] X. S. Li, C. W. Magnuson, A. Venugopal, R. M. Tromp, J. B. Hannon, E. M. Vogel, L. Colombo, R. S. Ruoff, *J. Am. Chem. Soc.* **2011**, *133*, 2816.

[15] X. S. Li, W. W. Cai, L. Colombo, R. S. Ruoff, *Nano Lett.* **2009**, *9*, 4268.

[16] C. Mattevi, H. Kim, M. Chhowalla, *J. Mater. Chem.* **2011**, *21*, 3324.

[17] A. Srivastava, C. Galande, L. Ci, L. Song, C. Rai, D. Jariwala, K. F. Kelly, P. M. Ajayan, *Chem. Mater.* **2010**, *22*, 3457.

[18] Y. G. Yao, Z. Li, Z. Y. Lin, K.-S. Moon, J. Agar, C. Wong, *J. Phys. Chem. C* **2011**, *115*, 5232.

[19] Y. Zhang, L. Gomez, F. N. Ishikawa, A. Madaria, K. Ryu, C. Wang, A. Badmaev, C. W. Zhou, *J. Phys. Chem. Lett.* **2010**, *1*, 3101.

[20] M. Zheng, K. Takei, B. Hsia, H. Fang, X. Zhang, N. Ferralis, H. Ko, Y. L. Chueh, Y. Zhang, R. Maboudian, A. Javey, *Appl. Phys. Lett.* **2010**, *96*, 063110.

[21] K. L. Saenger, J. C. Tsang, A. A. Bol, J. O. Chu, A. Grill, C. Lavoie, *Appl. Phys. Lett.* **2010**, *96*, 153105.

[22] Q. K. Yu, J. Lian, S. Siriponglert, H. Li, Y. P. Chen, S. S. Pei, *Appl. Phys. Lett.* **2008**, *93*, 113103.

[23] N. Liu, L. Fu, B. Y. Dai, K. Yan, X. Liu, R. Q. Zhao, Y. F. Zhang, Z. F. Liu, *Nano Lett.* **2011**, *11*, 297.

[24] R. R. Nair, P. Blake, A. N. Grigorenko, K. S. Novoselov, T. J. Booth, T. Stauber, N. M. R. Peres, A. K. Geim, *Science* **2008**, *320*, 1308.

[25] M. S. Dresselhaus, A. Jorio, M. Hofmann, G. Dresselhaus, R. Saito, *Nano Lett.* **2010**, *10*, 751.

[26] L. M. Malard, M. A. Pimenta, G. Dresselhaus, M. S. Dresselhaus, *Phys. Rep.* **2009**, *473*, 51.

[27] J. Hass, F. Varchon, J. E. Millán-Otoya, M. Sprinkle, N. Sharma, W. A. de Heer, C. Berger, P. N. First, L. Magaud, E. H. Conrad, *Phys. Rev. Lett.* **2008**, *100*, 125504.

[28] A. Luican, G. H. Li, A. Reina, J. Kong, R. R. Nair, K. S. Novoselov, A. K. Geim, E. Y. Andrei, *Phys. Rev. Lett.* **2011**, *106*, 126802.

[29] J. J. Lander, H. E. Kern, A. L. Beach, *J. Appl. Phys.* **1952**, *23*, 1305.

[30] M. Eizenberg, J. M. Blakely, *J. Chem. Phys.* **1979**, *71*, 3467.

[31] R. Yang, L. C. Zhang, Y. Wang, Z. W. Shi, D. X. Shi, H. J. Gao, E. G. Wang, G. Y. Zhang, *Adv. Mater.* **2010**, *22*, 4014.

[32] I. Vlassiouk, M. Regmi, P. Fulvio, S. Dai, P. Datskos, G. Eres, S. Smirnov, *ACS Nano.* **2011**, *5*, 6069.